Catal Lett (2008) 125:123–129
DOI 10.1007/s10562-008-9526-1

Effect of Sodium in Ferrierite on Selective Catalytic Reduction of NO by Acetylene

Hui Pan · Xinping Wang · Na Xing · Zhiguan Liu

Received: 31 December 2007 / Accepted: 20 May 2008 / Published online: 10 June 2008

Abstract Influence of sodium in ferrierite (HFER) zeolite on selective catalytic reduction of NO by acetylene (C_2H_2-SCR) was investigated. NO_x-TPD and FT-IR indicated that small amount of sodium exchanged into the proton-form zeolite with an exchange level of about 11.8% is beneficial for the title reaction by accelerating active nitrate species formation on catalyst surface from NO_2 and by suppressing the reductant combustion. Nevertheless, no further improved catalytic performance in C_2H_2-SCR could be observed by a larger amount of sodium exchanged into HFER due to some inactive nitrate species formed on the zeolite. Instead, activity of the zeolite for C_2H_2-SCR was drastically reduced, since the capacity of the zeolite for catalyzing NO oxidation and accelerating active NO^+ species formation was remarkably depressed.

Keywords Sodium · FER · Nitrosonium ions · Nitrate · Acetylene · Selective catalytic NO reduction

1 Introduction

Selective catalytic reduction of NO with hydrocarbons (HC-SCR) in excess oxygen has received much attention recently because of its potential application to mobile lean-burn engines [1–4]. Since the HC-SCR was first studied over Cu-ZSM-5 catalysts by Iwamoto et al. [5], large number of investigations were reported over the zeolite based catalysts. Na and H form zeolites were usually used as precursors for preparation of the catalysts, and the activity of the zeolite for HC-SCR was reported to be strongly affected by the counter ions (H^+ or Na^+) in zeolites. For instance, it was reported that Ag-NaZSM-5 catalyst is more active than Ag-HZSM-5 for the selective catalytic reduction of NO by methane (CH_4-SCR) at 450 °C [6], and that Fe-ZSM-5 catalyst prepared from Na-ZSM-5 is far more active than that prepared from NH_4-ZSM-5 for selective catalytic reduction of NO by urea [7]. Similarly, high activity for the selective catalytic reduction of NO by propene (C_3H_6-SCR) on Ce-NaZSM-5 [8, 9] and for CH_4-SCR on Pt-Co-NaFER washcoated cordierite monolith [10] was obtained. Whereas, Brönsted acids have been suggested to be essential for HC-SCR over many catalytic systems (e.g. ZSM-5 modified by Pd, Ga, In, Ce and Ag) [11–18]. The authors found that Brönsted acids contributed to the aimed reaction in different steps. Also, Stakheev et al. have pointed out that protons in ZSM-5 are quite important for C_3H_6-SCR. They reported that exchange of partial protons by sodium with a level of 32% resulted in a nearly complete disappearance of the activity of the zeolite for oxidation of NO to NO_2, and a significant decrease of the activity for C_3H_6-SCR [19]. On the other hand, Satsumaon et al. has found that partially protonated alkaline-MOR is more active than the corresponding acidic zeolite for C_3H_6-SCR below 573 K. They attributed the high activity of the resulted zeolite to the higher concentration of NO_3^- that could be produced on the zeolite in the reaction conditions [20].

In this paper, a significant promotional effect of sodium in ferrierite zeolite on the reduction of NO with acetylene (C_2H_2-SCR) in the temperature range of 250–450 °C was reported and the mechanism of sodium ions contributing to the reaction was investigated in detail.

H. Pan · X. Wang (✉) · N. Xing · Z. Liu
State Key Laboratory of Fine Chemicals, Dalian University of Technology, 288#, Linggong Road 2, Dalian 116024, China
e-mail: dllgwxp@dlut.edu.cn

2 Experimental

HFER was obtained calcining NH_4-ferrierite zeolite (with Si/Al = 10, purchased from Zeolite Co.) at 500 °C in air for 6 h. Sodium exchanged zeolites were prepared by stirring 4 g of HFER in 50 mL of 0.2 M aqueous sodium nitrate solution at 80 °C for a desired period of time. The resulting materials were then filtered, rinsed with deionized water, dried at 120 °C and calcined at 500 °C in air for 6 h. The composition of the zeolite samples thus obtained was determined by X-ray fluorescence (XRF) on SRS-3400 spectrometer.

To prepare some ferrierite samples with the desired sodium content in the range of 0.2–5%, HFER was impregnated by sodium nitrate solution with some certain concentration over night, and the resulting materials were dried at 120 °C, calcined at 500 °C in air for 6 h. The zeolites obtained in this way are denoted as *x*Na/HFER, where *x* indicates the weight percentage of Na_2O in the zeolites.

All of the zeolites were then palletized, crushed and sieved to a size of 20–40 mesh before use.

Temperature-programmed desorption of NO and NO_2 (NO_x-TPD) was conducted on a homemade setup with an electrochemical NO_x analyzer (ACY301-B). After saturated co-adsorption of 200 ppm NO and 10% O_2 in N_2 at 40 °C and a purge with N_2 for 2 h, the sample (0.2 g) was heated to 500 °C in N_2 at 10 °C/min, during which the effluent gas was continuously monitored as a function of temperature.

In situ FTIR spectra were recorded in a quartz IR cell equipped with CaF_2 windows on Nicolet 360 FTIR spectrophotometer, by accumulating 32 scans at a resolution of 2 cm^{-1}. Before each experiment, zeolite self-supporting wafer was activated in situ at 500 °C in N_2 flow. Co-adsorption of NO and O_2 was conducted by exposing the sample to 1,000 ppm NO + 10% O_2 in N_2 at the desired temperature. Reactivity of nitrous species towards acetylene was studied in the following procedure: flow a gas mixture of 1,000 ppm NO +10% O_2 in N_2 through IR cell for 30 min (pre-adsorption); evacuate the cell briefly and then flow a gas mixture of 500 ppm C_2H_2 + 10% O_2 in N_2 through the IR cell, during which steady or transient FTIR spectra were recorded. To obtain IR spectra of surface species, the corresponding adsorption spectra of both wafer-self and adsorbate gas were subtracted from the recorded FTIR spectra.

Activity of the zeolite (0.2 g) for NO oxidation was tested in a quartz reactor (4 mm i.d.). Gas mixture of 200 ppm NO + 10% O_2 in N_2 was fed to the reactor at a total flow rate of 100 mL/min. Produced NO_2 and unreacted NO in the outlet gas were monitored by a NO_x analyzer (ACY301-B).

C_2H_2 oxidation by O_2 over 0.2 g of the catalyst was conducted in a quartz reactor (i.d. 4 mm) at each desired temperature. A gas mixture of 800 ppm C_2H_2 + 10% O_2 in He was fed to the reactor at a total flow rate of 50 mL/min and the effluent gas was analyzed by GC with FID (without separating column).

C_2H_2-SCR reaction was carried out in a quartz reactor (4 mm i.d.) by feeding a gas mixture of 1,600 ppm NO + 800 ppm C_2H_2 + 9.95% O_2 in He at a total flow rate of 50 mL/min to 0.2 g of catalyst. NO conversion was calculated from the amount of N_2 produced, which was analyzed using a gas chromatograph (HP 6890) equipped with a capillary column (HP-PLOT/zeolite, 30 m × 0.32 mm, 12 μm).

3 Results and Discussion

3.1 Composition of the Zeolites

The chemical composition of the ion-exchanged zeolites analyzed by XRF is given in Table 1. The content of sodium in Na(2)HFER was about twice of that in Na(1)HFER, which was well supported by Fig. 1. The band at 3,595 cm^{-1} due to Brönsted acid hydroxyl groups [20] on HFER decreased in intensity with the increase of sodium in the zeolite samples, and correspondingly, a new band at 3,695 cm^{-1} representing hydroxyl groups located on Na^+ cations [21] became visible. On the other hand, the band at 3,647 cm^{-1} due to hydroxyl groups attached to extra framework alumina [22] almost did not change. The results indicate that sodium incorporated into the zeolites replaced some Brönsted acid sites, and combined with H_2O in zeolites. No bands due to $NaNO_3$ [23] could be observed by FTIR in the region of 1,350–1,450 cm^{-1}.

Table 1 Composition of the ion-exchanged zeolites

Zeolites	Exchanging time (h)[a]	Na_2O (wt.%)	Al_2O_3 (wt.%)	SiO_2 (wt.%)	Na/Al (mol%)
HFER	None	0	7.70	88.3	0
Na(1)HFER	4 × 1	0.584	7.87	88.2	11.8
Na(2)HFER	24 × 3	1.460	7.64	88.6	31.5

[a] Exchanging time = hours spent in exchanging once × times

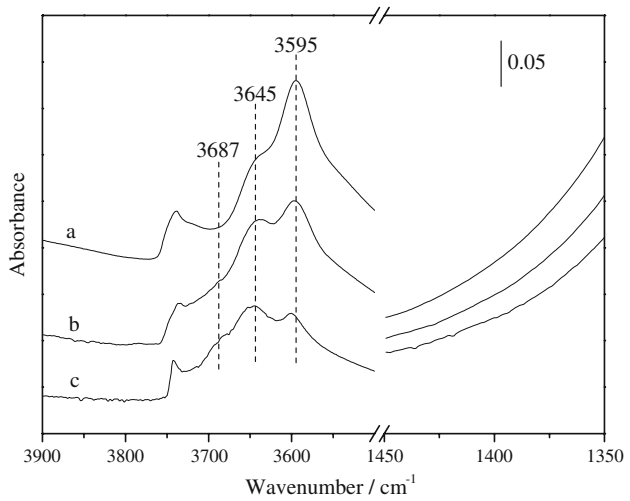

Fig. 1 FT-IR spectra of the zeolites at 250 °C: HFER (**a**), Na(1)HFER (**b**), Na(2)HFER (**c**)

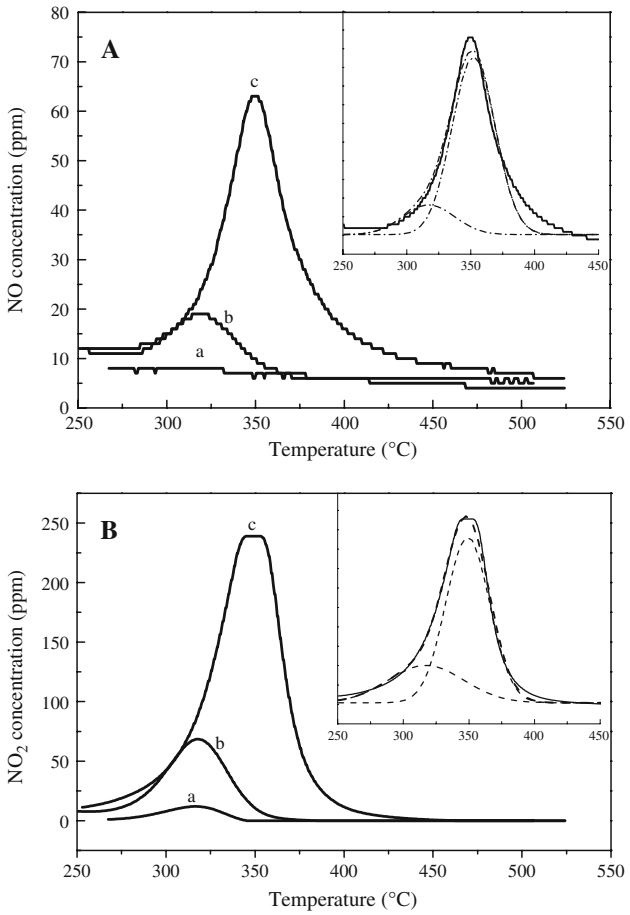

Fig. 2 TPD profiles of NO (**A**) and NO_2 (**B**) in N_2 after saturated co-adsorption of NO with O_2 on HFER (a), Na(1)HFER (b) and Na(2)HFER (c). The insert shows the simulation of NO or NO_2 desorbed at different temperature on Na(2)HFER

3.2 Co-adsorption of NO and O_2 on the Zeolites

NO and NO_2 desorption after saturated co-adsorption of NO and O_2 on the zeolites, were recorded as a function of temperature (Fig. 2). Desorption peaks of NO and NO_2 on HFER and Na(1)HFER zeolites centered at 317 °C, while those from Na(2)HFER zeolite behaved as a large broad one that can be deconvolved into two peaks centered at 317 and 350 °C, respectively (shown in the inserts). The new peaks centered 350 °C of NO and NO_2 may be associated with a type of nitric species produced by large amount of sodium incorporated into the zeolite. Accordingly, about 0.0069, 0.079 and 0.42 mmol/g of NO_x desorption from HFER, Na(1)HFER and Na(2)HFER were respectively calculated by integrating the desorption peaks of NO and NO_2 (in Fig. 2) in range of 275–425 °C. This order is in good accordance with the sodium content of zeolites, which means that sodium ions in the zeolites are favorable for NO_x storage under the experimental conditions. Nevertheless, the total desorption amount (0.083 mmol/g) of NO and NO_2 on Na(2)HFER zeolite at around 317 °C (as shown in the inserts) was almost the same as that on Na(1)HFER (0.079 mmol/g). It means that the nitric species associated with the NO_x desorption at 317 °C can not be significantly increased by excess sodium (>11.8% in Na/Al ratio) in the zeolite.

The adsorption states of NO and/or NO_2 on the zeolites in the presence of O_2 were characterized by FTIR (Fig. 3).

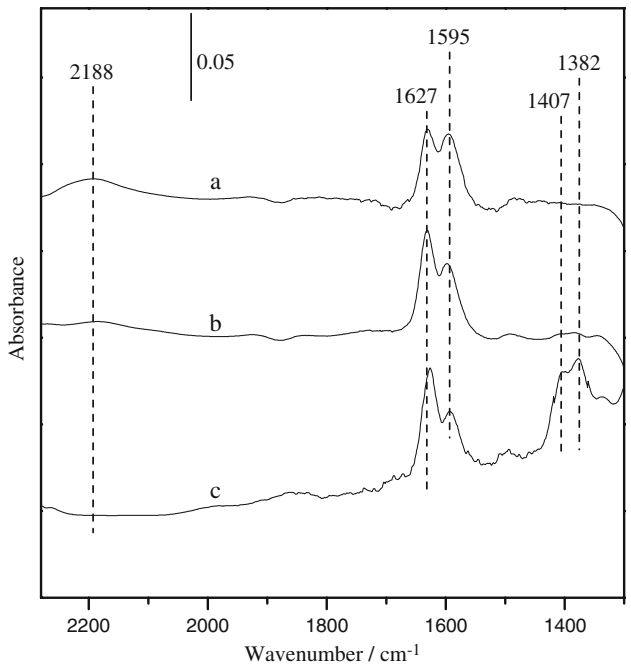

Fig. 3 Steady state in situ FTIR of surface species on HFER (**a**), Na(1)HFER (**b**) and Na(2)HFER (**c**) at 250 °C in 1,000 ppm NO + 10% O_2 + N_2

After saturated co-adsorption of NO and O_2, all of the zeolites gave a band at 1,627 cm^{-1} due to bridging nitrates [22, 24–27] and a band at 1,595 cm^{-1} due to bidentate nitrates [26–28]. Therefore, the two types of nitrate species can be associated with the NO_x desorption at 317 °C in the NO_x-TPD. On the other hand, two new bands at 1,407 and 1,382 cm^{-1} were observed in FTIR on Na(2)HFER zeolite, which can be assigned to the vibration of nitrates located on sodium ions [22, 25, 29]. This type of nitrate species may be associated with the large desorption peaks of NO and at NO_2 at 350 °C in NO_x-TPD.

Figure 4 shows reactivity of the nitric species on Na(2)HFER towards reduction by acetylene at 250 °C. The bands at 1,627 and 1,595 cm^{-1} disappeared upon exposing the zeolites to $C_2H_2 + O_2$ within 5 min. Concomitantly, bands at 1,682 cm^{-1} due to carbonyl-containing compound [ν(C=O)] [30] and 1,625 cm^{-1} due to δ (H_2O) vibration of water [31] appeared and increased in intensity. The results indicate that the two types of nitrate species are rather reactive towards the reductant at 250 °C. Compared to those on Na(2)HFER, the bands at 1,627 and 1,595 cm^{-1} disappeared more rapidly on HFER and Na(1)HFER zeolites under the same experimental conditions (not shown). No significant change in intensity of bands at 1,407 and 1,382 cm^{-1} could be observed during the exposure of Na(2)HFER zeolite to $C_2H_2 + O_2$ for 30 min. It reveals that the nitrate species with the bands at 1,407 and

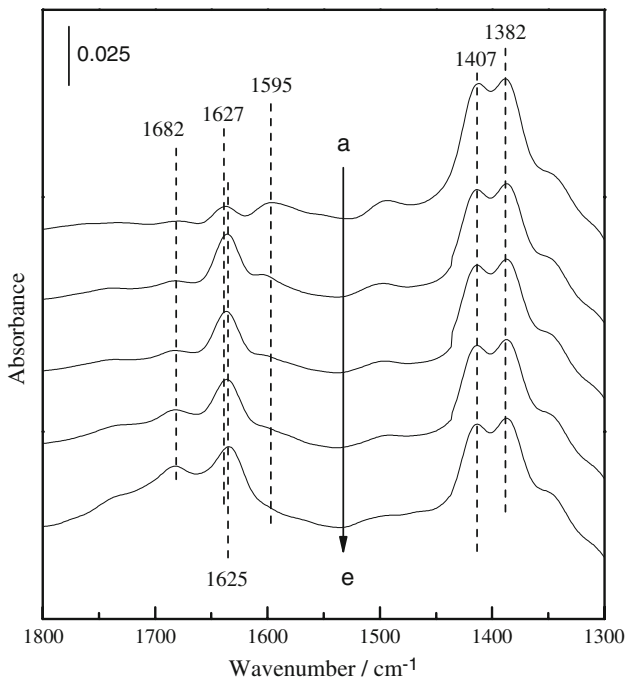

Fig. 4 Transient FTIR spectra of surface species on Na(2)HFER at 250 °C: a brief evacuation after saturated co-adsorption of NO + O_2 (**a**), subsequently exposed to $C_2H_2 + O_2$ for 1 min (**b**), 5 min (**c**), 10 min (**d**), 30 min (**e**)

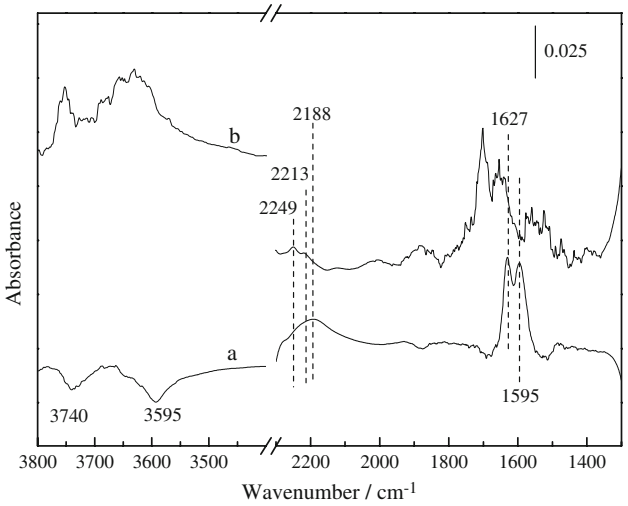

Fig. 5 In situ FTIR of species formed on HFER at 250 °C in flow of 1,000 ppm NO + 10% $O_2 + N_2$ (**a**) and in 1,000 ppm NO + 500 ppm C_2H_2 + 10% $O_2 + N_2$ (**b**)

1,382 cm^{-1} on Na(2)HFER is inert to the reductant. In other words, this type of nitrate species just acts as a spectator in C_2H_2-SCR.

An in situ FTIR spectrum of the surface species on HFER after saturated co-adsorption of NO and O_2 is presented in Fig. 5 (spectrum a). Besides of the bands at 1,627 and 1,595 cm^{-1}, a band at 2,188 cm^{-1} together with two negative bands at 3,740 cm^{-1} due to Si–OH silanols [32] and 3,595 cm^{-1} due to hydroxyls on bridged SiOAl [20] (i.e., the sites of protons) appeared during NO + O_2 co-adsorption. This spectrum quite resembles that obtained by Hadjiivanov et al. [31], in which a band at 2,133 cm^{-1} together with the negative bands at 3,740 and 3,600 cm^{-1} were observed after NO + O_2 co-adsorption on HZSM-5 zeolite at room temperature. The authors have assigned the band at 2,133 cm^{-1} to NO^+, and proposed a formation route as

$$NO + O_2 + H^+ \rightarrow NO^+ + H_2O$$

Accordingly, the band at 2,188 cm^{-1} observed on HFER in our case can be reasonably attributed to NO^+ located on the proton sites. As characterized by the FTIR in the Fig. 3 (band at 2,188 cm^{-1}), the NO^+ species produced on the zeolites in population, after saturated co-adsorption of NO and O_2 at 250 °C, has a direct relation with the amount of protons in the zeolites. The result supports well the above formation route of NO^+ proposed by Hadjiivanov et al. Quite different from the spectrum a, the steady spectrum b could not give the band at 2,188 cm^{-1} at the same temperature when acetylene was introduced into the gas mixture. Instead, bands at 2,249 cm^{-1}due to isocyanate (–NCO) [33–37] and 2,213 cm^{-1} due to cyanide (–CN) species [36–38] were observed. The result can be reasonably interpreted as follows: NO^+ is so active towards the

reductant at the temperature that it is reduced by the reactant right away, once produced from NO_x adsorption under the reaction conditions. In literature, NO^+ was proposed to be an intermediate over H-mordenite [39] in C_3H_6-SCR. Also, it was suggested to be active surface intermediate to form N_2 in CH_4-SCR over Co-, Co, Pt-, and H-mordenite [40]. Clearly, the explanation concerning high reactivity of NO^+ species towards C_2H_2-SCR is also supported by the literature. Besides of the band at 2,188 cm^{-1}, the bands at 1,627 and 1,595 cm^{-1} were not detected in spectrum b, indicating again that the two types of nitrates species are also reactive towards C_2H_2-SCR.

3.3 NO Oxidation Catalyzed by the Zeolites

As NO oxidation to NO_2 is an indispensable step for the formation of nitric species (NO^+, nitrates), the activity of the ion-exchanged zeolites for NO oxidation to NO_2 was investigated at 250–450 °C (in Fig. 6). It is obvious that the partial substitution of protons by sodium ions suppressed the activity of FER zeolites for the reaction. With sodium content increasing, the conversion of NO to NO_2 over FER zeolites remarkably decreased.

3.4 C_2H_2 Combustion Influenced by Sodium in the Zeolites

Activity of the ion-exchanged zeolites for acetylene oxidation by O_2 is depicted in Fig. 7. The combustion of C_2H_2 was substantially inhibited by sodium in the zeolites. For instance, conversion of C_2H_2 to CO_2 over HFER was 71%, whereas it drastically decreased to 48% over Na(1)HFER at 350 °C.

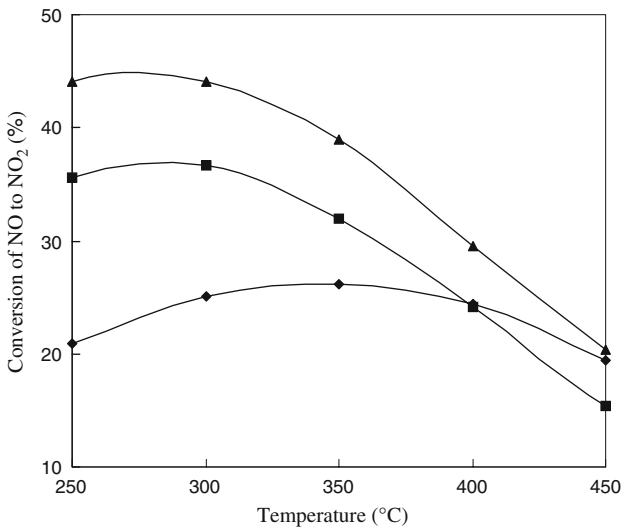

Fig. 6 Catalytic performance of HFER (▲), Na(1)HFER (■) and Na(2)HFER (◆) in oxidation of NO with O_2

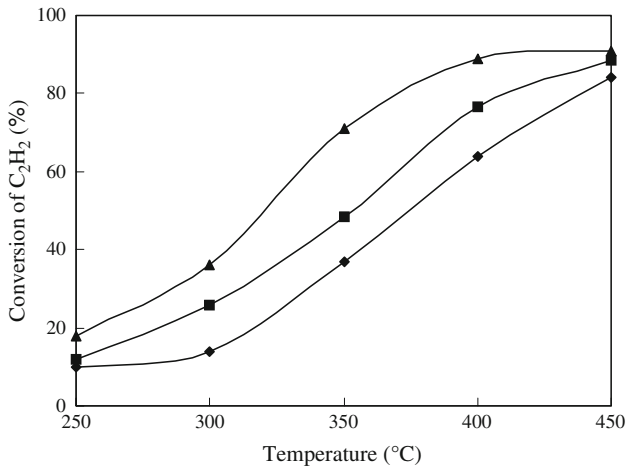

Fig. 7 Combustion of C_2H_2 over HFER (▲), Na(1)HFER (■) and Na(2)HFER (◆) at different temperature

3.5 Catalytic Activity of the Zeolites for C_2H_2-SCR

The catalytic performance of HFER, Na(1)HFER and Na(2)HFER zeolites in C_2H_2-SCR is depicted in Fig. 8. At 250 °C, HFER zeolite gave higher NO conversion to N_2 compared to Na(1)HFER, which may be the result that more active NO^+ species in population could be produced on HFER than on Na(1)HFER as characterized by in situ FTIR shown in Fig. 3 (spectrum a and b) at the same reaction conditions. When the reaction temperature increased to 350 °C, 91% NO conversion over Na(1)HFER zeolite was achieved, which is higher than that obtained over HFER at the same temperature. The opposite order in

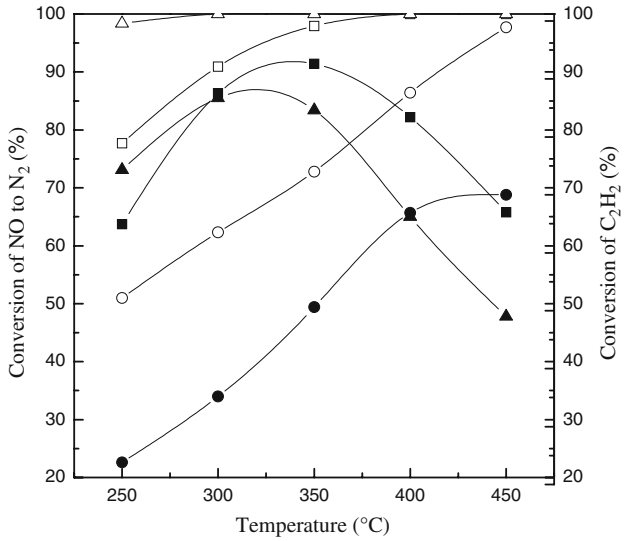

Fig. 8 NO conversion to N_2 (open symbols) and C_2H_2 conversion (closed symbols) over HFER (▲, Δ), Na(1)HFER (■, □), Na(2)HFER (●, ○) as a function of reaction temperature in C_2H_2-SCR

activity at different temperature (250 and 350 °C) can be interpreted by the supposition that different nitric species predominantly contributes to the title reaction at different temperature: NO^+ is mainly responsible for the title reaction at 250 °C, whereas the bridging and bidentate nitrate species (1,627 and 1,595 cm^{-1}) become the main active species contributing to the title reaction at 350 °C. As shown in Fig. 3, although more active NO^+ species could be produced on HFER than on Na(1)HFER and Na(2)HFER, much more active nitrate species in population could be formed on Na(1)HFER than on HFER in the same conditions, which is supported by the larger desorption of NO and NO_2 at 317 °C for Na(1)HFER compared to HFER in NO_x-TPD. Hence, the higher activity of Na(1)HFER zeolite for the title reaction than HFER above 300 °C can be reasonably attributed to the improved active nitrate species formation capacity of the zeolite by small amount of sodium incorporation into the zeolite.

On the contrary, large amount of sodium incorporated into HFER significantly depressed the activity of the zeolite for C_2H_2-SCR. As shown in Fig. 8, Na(2)HFER even behaved rather worse catalytic performance in C_2H_2-SCR than HFER. The result could be reasonably interpreted by the significantly depressed activity of the zeolite for NO oxidation to NO_2 due to large amount of sodium incorporation into the zeolite. As discussed in section 3.3, NO oxidation to NO_2 is an indispensable step for the nitric species formation on the zeolite, which is catalyzed by protons presenting in the zeolite. Thus, the replacement of protons by more than some certain amount of sodium may make the rate of active nitric species formation decrease remarkably, so that C_2H_2-SCR is restricted by the NO oxidation step. Furthermore, as discussed in Sect. 3.2, no more active nitric species, but the inactive nitrate species on the zeolite (Figs. 3 and 4) was produced by more than 11.8% of the sodium incorporation. The results strongly indicate that the amount of sodium in the zeolite must be so appropriate that the active nitric species formation capacity of the zeolite can be effectively improved and the activity of zeolite for NO oxidation can be retained in some extent as well.

In the temperature range of 300–400 °C, higher selectivity towards the title reaction was obtained on Na(1)HFER compared to that on HFER, which can be deduced from the higher NO conversion and lower C_2H_2 conversion over the former than over the latter. The results may be associated with the depression of sodium ions on C_2H_2 combustion, as discussed in Sect. 3.4.

For the *x*Na/HFER catalyst samples prepared by impregnating HFER in sodium nitrate, similar regularity representing that small amount of sodium incorporated into HFER zeolite is favorable for C_2H_2-SCR was obtained. As shown in Fig. 9, 0.2%Na/FER gave the highest NO conversion to N_2 at 350 °C among *x*Na/HFER samples.

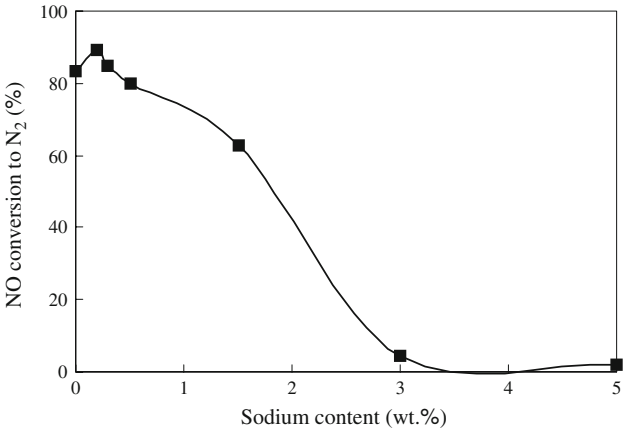

Fig. 9 Conversion of NO to N_2 at 350 °C in the C_2H_2-SCR as a function of sodium content of Na/FER

4 Conclusions

Formation of the active nitric species (NO^+, bridging and bidentate nitrate) is a crucial step for C_2H_2-SCR over FER zeolite. Small amount of sodium incorporated into the zeolite (with an exchange level of protons less than 11.8%) significantly promoted the activity of the zeolite for C_2H_2-SCR by improving the active nitric species formation and suppressing the reductant combustion over the zeolite. Contrarily, the exchange of proton by sodium with the higher level (e.g. 31.5%) resulted in inactive nitrate species formation on the zeolite. Furthermore, the over-exchange led to the activity of the zeolite for NO oxidation diminishing and the active NO^+ species formation capacity of the zeolite decreasing. As a consequence, the activity of the zeolite for C_2H_2-SCR drastically was depressed by sodium over-exchanged in the zeolite.

Acknowledgment Support was provided by the National Natural Science Foundation of China (grant No. 20677006).

Reference

1. Fokema MD, Ying JY (2001) Catal Rev 43(1&2):1
2. Burch R, Breen JP, Meunier FC (2002) Appl Catal B 39:283
3. Chen H, Sun Q, Wen B, Yeom Y, Weitz E, Sachtler WMH (2004) Catal Today 96:1
4. Gómez-García MA, Pitchon V, Kiennemann A (2005) Environ Int 31:445
5. Iwamoto M, Yahiro H, Yu-u Y, Shundo S, Mizuno N (1990) Shokubai 32:430
6. Shi C, Cheng M, Qua Z, Yang X, Bao X (2002) Appl Catal B 36:173
7. Sullivan JA, Keane O (2005) Appl Catal B 61:244
8. Yokoyama C, Misono M (1994) Catal Today 22:59
9. Yokoyama C, Misono M (1996) J Catal 160:95
10. Boix AV, Zamaro JM, Lombardo EA, Miró EE (2003) Appl Catal B 46:121
11. Loughran CE, Resasco DE (1995) Appl Catal B 7:113

12. Kikuchi E, Yogo K (1994) Catal Today 22:73
13. Y. Nishizaka, M. Misono (1994) Chem Lett 2237
14. Li Y, Armor JN (1994) J Catal 145:1
15. Narbeshuber TF, Brait A, Seshan K, Lercher JA (1997) J Catal 172:127
16. Berndt H, Schütze F-W, Richter M, Sowade T, Grünert W (2003) Appl Catal B 40:51
17. Shibata J, Takada Y, Shichi A, Satokawa S, Satsuma A, Hattori T (2004) Appl Catal B 54:137
18. Gutierrez L, Ulla MA, Lombardo EA, Kovács A, Lónyi F, Valyon J (2005) Appl Catal A 292:154
19. Stakheev AY, Lee CW, Park SJ, Chong PJ (1996) Catal Lett 38:271
20. Satsuma A, Yamada K, Sato K, Shimizu K, Hattori T (1997) Catal Lett 45:267
21. Stakheev AYu, Lee CW, Park SJ, Chong PJ (1996) Appl Catal B 9:65
22. Li G, Larsen SC, Grassian VH (2005) Catal Lett 103:23
23. Sedlmair C, Gil B, Seshan K, Jentys A, Lercher JA (2003) Phys Chem Chem Phys 5:1897
24. Sedlmair C, Seshan K, Jentys A, Lercher JA (2003) J Catal 214:308
25. Li G, Larsen SC, Grassian VH (2005) J Mol Catal A 227:25
26. Yu Y, He H, Feng Q, Gao H, Yang X (2004) Appl Catal B 49:159
27. Yu Q, Wang X, Xing N, Yang H, Zhang S (2007) J Catal 245:124
28. He H, Zhang C, Yu Y (2004) Catal Today 90:191
29. Szanyi J, Kwak JH, Peden CHF (2004) J Phys Chem B 108:3746
30. Yeom YH, Li M, Sachtler WMH, Weitz E (2006) J Catal 238:100
31. Hadjiivanov K, Saussey J, Freysz JL, Lavalley JC (1998) Catal Lett 52:103
32. Gerlach T, Schütze FW, Baerns M (1999) J Catal 185:131
33. Shimizu K, Shibata J, Yoshida H, Satsumal A, Hattori T (2001) Appl Catal B 30:151
34. Satsuma A, Shimizu K (2003) Prog Energy Combust Sci 29:71
35. Kameoka S, Ukisu Y, Miyadera T (2000) Phys Chem Chem Phys 2:367
36. Bion N, Saussey J, Hedouin C, Seguelong T, Daturi M (2001) Phys Chem Chem Phys 3:4811
37. Haneda M, Joubert E, Ménézo J-C, Duprez D, Barbier J, Bion N, Daturi M, Saussey J, Lavalley J-C, Hamadac H (2001) J Mol Catal A 175:179
38. Haneda M, Bion N, Daturi M, Saussey J, Lavalley J-C, Duprez D, Hamada H (2002) J Catal 206:114
39. Cant NW, Liu IOY (2000) Catal Today 63:133
40. Lónyi F, Valyon J, Gutierrez L, Ulla MA, Lombardo EA (2007) Appl Catal B 73:1